




## *Pomacentrus andamanensis*, a new species of damselfish (Teleostei: Pomacentridae) from the Andaman Sea, Indian Ocean

GERALD R. ALLEN


Department of Aquatic Zoology, Western Australian Museum,  
Locked Bag 49, Welshpool DC, Perth, Western Australia 6986

 <https://orcid.org/0000-0002-4661-4898> E-mail: [gerry.tropicalreef@gmail.com](mailto:gerry.tropicalreef@gmail.com)

MARK V. ERDMANN

Conservation International Asia-Pacific Marine Program, University of Auckland,  
23 Symonds St., Auckland 1020 New Zealand

California Academy of Sciences, Golden Gate Park, San Francisco, CA 94118, USA

 <https://orcid.org/0000-0002-3644-8347> E-mail: [mverdmann@gmail.com](mailto:mverdmann@gmail.com)

ENEX YUNI NINGSIH

Biodiversitas Indonesia (BIONESIA), Jl. Tukad Balian No. 121, Denpasar 80226, Bali, Indonesia

E-mail: [yuniartiningsih3@gmail.com](mailto:yuniartiningsih3@gmail.com)

### Abstract

A new damselfish species, *Pomacentrus andamanensis* n. sp., is described from 45 specimens, 19.8–64.3 mm SL, collected from Indian Ocean coral reefs, in the Andaman Sea off western Thailand. It also occurs in the Andaman Islands, Myanmar, and the northwestern tip of Sumatra, on the basis of collections (with tissue sampling), underwater photographs, and observations. It is a sibling species of *Pomacentrus amboinensis* from the Western Pacific Ocean, but differs from it and the Micronesian species of the complex, *Pomacentrus bipunctatus*, primarily in the adult color pattern, in particular a conspicuous ocellus on the rear dorsal fin in adults, which is only found on juveniles of the other species. Most meristic values are the same, but the range of total gill rakers differs, although with some overlap. An analysis of the mtDNA control-region sequences for the new species shows a deep divergence of 21% from 7 populations of Pacific *P. amboinensis*.

**Key words:** taxonomy, ichthyology, phylogenetics, coral reef fishes, Thailand, Myanmar, Indonesia, Indo-Pacific

**Citation:** Allen, G.R., Erdmann, M.V. & Ningsih, E.Y. (2020) *Pomacentrus andamanensis*, a new species of damselfish (Teleostei: Pomacentridae) from the Andaman Sea, Indian Ocean. *Journal of the Ocean Science Foundation*, 36, 38–48.

**doi:** <https://doi.org/10.5281/zenodo.4340748>

**urn:lsid:zoobank.org:pub:E7AC1FFF-2EB1-4216-B01D-0D34922230BE**

**Date of publication of this version of record:** 17 December 2020

## Introduction

Damselfishes of the family Pomacentridae form an integral part of the tropical and warm temperate shorefish fauna globally. They are among the most conspicuous diurnal inhabitants of coral reefs, both in number of species and individuals. There are currently 423 valid species recognized (Fricke et al. 2020a), but many taxa are yet to be explored phylogenetically. *Pomacentrus* Lacepède, 1802 of the Indo-Pacific region, with 79 species (Fricke et al. 2020b), is the second largest genus in the family after *Chromis* Cuvier, 1802 (105 species). We describe here a new species from the Andaman Sea that has been considered a geographic variant of the widely distributed western Pacific species, *Pomacentrus amboinensis* (Bleeker, 1868) (Allen 1991, Allen & Erdmann 2012).

## Materials and Methods

Type specimens are deposited at the Royal Ontario Museum, Toronto (ROM) and the Western Australian Museum, Perth (WAM). Other material is from BPBM (Bishop Museum, Honolulu), CAS (California Academy of Sciences), and USNM (United States National Museum of Natural History, Washington, DC).

Lengths of specimens are given as standard length (SL) measured from the anterior end of the upper lip to the base of the caudal fin (posterior edge of the hypural plate); head length (HL) is measured from the same anterior point to the posterior edge of the opercle flap; body depth is the maximum depth taken vertically between the belly and base of the dorsal-fin spines; body width is the maximum width just posterior to the gill opening; snout length is measured from the anterior end of the upper lip to the anterior edge of the eye; orbit diameter is the horizontal fleshy diameter, and interorbital width the least fleshy width; upper jaw length is taken from the front of the upper lip to the posterior end of the maxilla; caudal-peduncle depth is the least depth, and caudal-peduncle length is the horizontal distance between verticals at the rear base of the anal fin and the caudal-fin base; lengths of fin spines and rays are measured to their extreme bases (i.e. not from the point where the ray or spine emerges from the basal scaly sheath); caudal-fin length is the horizontal length from the posterior edge of the hypural plate to a vertical at the tip of the longest ray; caudal concavity is the horizontal distance between verticals at the tips of the shortest and longest rays; pectoral-fin length is the length of the longest ray; pelvic-fin length is measured from the base of the pelvic-fin spine to the filamentous tip of the longest soft ray; pectoral-fin ray counts include the small splint-like uppermost rudimentary ray; only the tube-bearing anterior lateral-line scales are counted; a separate count is given for the deeply pitted scales occurring in a continuous series midlaterally on the caudal peduncle; gill-raker counts include all rudiments and are presented as separate counts for the upper and lower limbs as well as a combined count; the last fin ray element of the dorsal and anal fins is usually branched near the base and is counted as a single ray. Counts and proportions are holotype (range for the paratypes, mean of all).

Mitochondrial DNA sequences were obtained from 7 specimens from the Andaman Islands and 41 specimens of *P. amboinensis* from 4 locations in Indonesia and Palawan in the Philippines, and 10 from Lizard and One Tree Islands in Queensland with 4 specimens of *Pomacentrus moluccensis* Bleeker, 1853 (outgroup) from the same locations (Bay et al. 2006). Specimens were fixed in 95% EtOH. Mitochondrial DNA was extracted using a 10% chelex solution (Walsh et al. 1991). Control region mtDNA was amplified using PCR (polymerase chain reaction) with forward primer CRA and reverse primer CRE from Lee et al. (1995). The PCR reaction was carried out in 25  $\mu$ L volume and 1  $\mu$ L of DNA template. Each reaction included 14.5  $\mu$ L of ddH<sub>2</sub>O, 2.5  $\mu$ L of 10x PCR Buffer (Applied Biosystems), 2.5  $\mu$ L of dNTPs (10 mM), 2.0  $\mu$ L of MgCl<sub>2</sub> solution (25 mM), 1.25  $\mu$ L of each primer (10  $\mu$ M), and 0.125  $\mu$ L of AmplyTaq Gold™ (Applied Biosystems). The PCR profile consisted of an initial denaturation (94°C for 10 min), 39 cycles of denaturation (94°C for 30 sec), annealing (48°C for 30 sec), and extension (72°C for 3 min), with final extension 72°C for 10 min. Following visualization of PCR product on 1% agarose gels stained with ethidium bromide, the PCR products were digested in 0.5  $\mu$ l of exonuclease I and 0.5  $\mu$ l of shrimp alkaline phosphatase for 30 minutes at 37°C followed by 15 minutes at 80°C. The PCR products were sequenced using both PCR primers using Big Dye® Chain Termination protocol. Samples were precipitated using 70% isopropanol and 70% ethanol prior to sequencing. Forward and reverse sequence analysis was conducted using MEGAX software (Kumar et al. 2018) and aligned with ClustalW. The best fitting substitution model was estimated with jModeltest 0.1.1 (Guindon & Gascuel 2003, Posada 2008). Phylogenetic trees were reconstructed using Bayesian methods in BEAST v1.10 (Suchard et al. 2018) HKY+G model with 10,000,000 replications, and 5,000 iterations used as the burn-in. Genetic distance was computed using Patristic (Fourment & Gibbs 2006).



*Pomacentrus andamanensis*, n. sp.

Eyespot Damselfish

urn:lsid:zoobank.org:act:4A545B11-4672-42B5-907E-332E2B318939

Figures 1, 2 & 5A–C; Tables 1 & 2

**Holotype.** WAM P.26506-001, 64.3 mm SL, Andaman Sea, Thailand, Surin Islands, 8.6667°, 97.6333°, 20–35 m, spear, G.R. Allen, 12 February 1979.

**Paratypes.** ROM 71364, 48.9 mm SL, Andaman Sea, Thailand, Phuket, Ko Hi, 7.7417°, 98.3756°, R. Winterbottom, 12 November 1993; ROM 71365, 13 specimens, 26.5–56.3 mm SL, Andaman Sea, Thailand, Phuket, Patong Beach, 7.9208°, 98.2711°, R. Winterbottom, 13 November 1993; ROM 71367, 2 specimens, 40.9 & 50.6 mm SL, Andaman Sea, Thailand, Phuket, Ko Racha Noi, 7.4708°, 98.3264°, R. Winterbottom, 18 November 1993; ROM 71368, 11 specimens, 28.3–55.2 mm SL, Andaman Sea, Thailand, Phuket, Ko Racha Noi, 7.4708°, 98.3264°, R. Winterbottom, 18 November 1993; ROM 71369, 37.5 mm SL, Andaman Sea, Thailand, Phuket, Ko Racha Yai, 7.5833°, 98.3625°, R. Winterbottom, 19 November 1993; ROM 71370, 33.4 mm SL, Andaman Sea, Thailand, Phuket, Ko Racha Yai, 7.5861°, 98.3681°, R. Winterbottom, 25 November 1993; ROM 71371, 3 specimens, 49.0–58.3 mm SL, Andaman Sea, Thailand, Phuket, Ko Hi, 7.5861°, 98.3681°, R. Winterbottom, 26 November 1993; ROM 71372, 4 specimens, 28.3–43.3 mm SL, Andaman Sea, Thailand, Similan Island, 8.6608°, 97.6775°, R. Winterbottom, 14 December 1993; ROM 71596, 3 specimens, 19.8–61.4 mm SL, Andaman Sea, Thailand, Phuket, Ko Doc Mai, 7.7978°, 98.5333°, R. Winterbottom, 15 November 1993; WAM P. 226504-002, 4 specimens, 54.8–60.8 mm SL, Andaman Sea, Phuket, Ko Hi, 7.7500°, 98.3667°, 4–8 m, spear, G.R. Allen, 7 February 1979; WAM P.26506-017, 60.4 mm SL, collected with holotype.

**Diagnosis.** Dorsal-fin elements XIII,14–15; anal-fin elements II,14–16 (usually 15); pectoral-fin rays 16–18 (usually 17); tubed lateral-line scales 16–19 (usually 17 or 18); total gill rakers on first arch 20–23 (rarely 20); body depth 1.9–2.1 (mean 2.0) in SL; scales absent on preorbital and suborbital; lower margin of suborbital series with 7–13 serrae; color in life pale lavender to bluish gray on upper two-thirds of body and dorsal head, otherwise



**Figure 1.** *Pomacentrus andamanensis* n. sp., approx. 60 mm SL, Similan Islands, Thailand (G.R. Allen).

yellowish including fins; small blue spots on body scales, large lavender spots and bands on side of head, greenish spot on upper opercle near lateral-line origin, small blackish spot at base of uppermost pectoral-fin rays, and blue to lavender stripes and spots on dorsal and anal fins; a conspicuous ocellus on the rear dorsal fin in both juveniles and adults.

**Description.** Dorsal-fin elements XIII,14 (14–15); anal-fin elements II,15 (14–16); all dorsal- and anal-fin soft rays branched, last to base; pectoral-fin rays 17 (16–18), uppermost two and lowermost ray unbranched; pelvic-fin rays I,5; principal caudal-fin rays 15, median 13 branched, upper procurrent rays 3 (3–5), lower procurrent rays 4 (3–4); scales in longitudinal series 27; tubed lateral-line scales 18 (16–19); posterior midlateral scales with a pore or deep pit (in continuous series), 8 (3–8); scales above lateral line to origin of dorsal fin 3; scales above lateral line to base of middle dorsal-fin spine 1.5; scales below lateral line to origin of anal fin 7.5; gill rakers 7 + 15 (6–8 + 13–16), total rakers 22 (20–23); pseudobranch filaments 14 (14–15); total vertebrae 26 (6 specimens).

Body ovate, depth 2.0 (1.9–2.1, 2.0) in SL, and compressed, width 2.5 (2.3–3.0, 2.6) in body depth; HL 3.3 (3.1–3.4, 3.2) in SL; dorsal profile of head evenly rounded from dorsal-fin origin to snout; snout length 3.5 (3.3–4.0, 3.6) in HL; orbit diameter 3.3 (2.8–3.4, 3.1) in HL; interorbital space convex, width 3.5 (3.0–3.6, 3.3) in HL; caudal-peduncle depth 2.0 (2.0–2.2, 2.1) in HL; caudal-peduncle length 3.3 (2.5–3.7, 3.0) in HL.

Mouth terminal, small, and oblique, forming an angle of about 25–30° to horizontal axis of head and body; maxilla reaching a vertical slightly beyond anterior edge of eye, upper-jaw length 3.4 (3.2–3.7, 3.5) in HL; teeth of jaws uniserial posteriorly, becoming biserial at front of jaws with additional slender buttress teeth in spaces between main row of larger teeth; teeth incisiform to conical, about 30–40 in main row of each jaw (excluding buttress teeth). Tongue triangular with rounded tip. Gill rakers long and slender, longest on lower limb near angle, about two-thirds length of longest gill filaments. Nostril round with slightly raised rim, level with lower edge of pupil and about midway between anterior edge of eye and upper lip.

Opercle ending posteriorly in flat spine, tip obtuse, barely projecting from beneath a large scale; rear margin of preopercle with 18 serrae on left side of holotype (10–20); preorbital with single serra, separated by rounded notch from suborbital series; lower margin of suborbital series with 10 (7–13) serrae.

Scales finely ctenoid, head scaled except lips and tip of snout, preorbital (lacrimal) and suborbital naked; scaly sheath at base of dorsal and anal fins, about 85–90% pupil width at base of dorsal fin and about the same width at middle part of anal fin, tapering on anteriormost and posteriormost sections; column of scales on each membrane of dorsal and anal fins, narrowing distally, those on spinous portion of dorsal fin progressively longer, reaching at least three-fourths distance to spine tips on posterior membranes, and covering as much as two-thirds of soft portion of dorsal and anal fins; small scales on caudal fin extending about two-thirds distance to posterior margin; small scales on basal third of pectoral fins; a cluster of several scales forming a median process, extending posteriorly from between base of pelvic fins, length one-third to two-thirds of pelvic-fin spine; axillary scale above base of pelvic-fin spine, its length one-third to two-thirds length of pelvic spine.

Origin of dorsal fin over second or third tubed lateral-line scale, predorsal distance 2.7 (2.3–2.9, 2.7) in SL; base of soft portion of dorsal fin contained 2.1 (1.8–2.4, 2.0) times in base of spinous portion; dorsal-fin spines gradually increasing in length to last spine; first dorsal-fin spine 3.2 (3.1–3.9, 3.4) in HL; seventh dorsal-fin spine 1.9 (1.7–2.2, 1.9) in HL; last dorsal-fin spine 1.7 (1.5–1.8, 1.7) in HL; membranes of spinous portion of dorsal fin moderately incised between spine tips; eighth dorsal-fin soft ray longest, 1.4 (1.2–1.4, 1.2) in HL; first anal-fin spine 4.1 (3.0–3.7, 3.5) in HL; second 1.9 (1.5–1.9, 1.7) in HL; longest (tenth or eleventh) anal-fin soft ray 1.3 (1.2–1.6, 1.3) in HL; caudal fin moderately forked with rounded lobes, length 2.9 (2.2–3.0, 2.8) in SL; fourth pectoral-fin ray longest, 3.4 (3.1–3.4, 3.3) in HL; pelvic-fin spine 1.7 (1.5–1.7, 1.6) in HL; first soft ray of pelvic fin forming filamentous tip (frequently damaged in preserved specimens), 3.0 (2.5–3.3, 2.8) in SL.

**Color in life.** (Figs. 1 & 5A–C) Generally pale lavender to bluish gray on upper two-thirds of body and dorsal part of head, yellow on snout, cheek, opercle, thorax, abdomen, and caudal peduncle; each body scale with 1–3 small blue spots; pale lavender markings on side of head and small greenish spot on upper opercle near lateral-line origin; iris yellow with a blue stripe near upper and lower edge, and a small blue spot behind upper rear corner of pupil; dorsal and anal fins yellowish with blue to pale lavender stripes and spotting, a prominent neon-green edged black spot between about sixth to eleventh soft-dorsal-fin rays; caudal and pelvic fins yellow with a fine blue outer margin; pectoral fins translucent with a small blackish spot at base of uppermost rays.

TABLE 1

Proportional measurements of selected type specimens of *Pomacentrus andamanensis*, n. sp.  
as percentages of the standard length

	holotype		paratypes							
	WAM P.26506	ROM 71596	WAM P.26504	WAM P.26506	WAM P.26504	ROM 71365	WAM P.26504	ROM 71371	ROM 71365	ROM 71368
Standard length (mm)	64.3	61.4	60.8	60.4	58.3	56.3	54.8	49.0	48.8	45.8
Body depth	47.9	50.1	49.5	50.8	52.1	49.8	49.5	50.9	50.5	49.9
Body width	18.9	19.2	19.1	18.6	22.2	20.0	17.5	20.9	20.4	18.1
Head length	30.3	31.0	31.3	30.7	30.9	32.7	32.0	31.0	31.8	32.4
Snout length	8.5	9.5	9.6	8.5	8.4	8.3	8.6	8.1	8.1	8.0
Orbit diameter	9.3	9.7	9.7	9.3	10.1	10.6	9.3	11.2	11.5	10.5
Interorbital width	8.6	10.0	10.2	8.7	8.7	9.7	9.3	9.6	9.1	10.7
Caudal-peduncle depth	15.5	15.1	16.0	15.5	14.7	14.6	15.4	14.6	14.6	15.0
Caudal-peduncle length	9.3	10.2	10.1	8.3	10.7	10.7	9.9	10.3	12.8	11.7
Upper jaw length	8.8	9.1	8.8	9.0	9.1	8.9	8.9	8.7	9.8	9.5
Predorsal length	36.1	36.1	37.3	36.9	43.4	37.7	38.1	37.1	38.1	37.2
Preanal length	69.7	66.0	71.7	66.4	70.4	65.9	67.9	67.7	66.9	65.4
Prepelvic length	40.9	40.2	41.4	38.8	43.7	39.9	40.1	38.6	38.7	38.6
Length dorsal-fin base	66.5	63.5	64.8	67.2	65.2	66.6	67.7	64.8	65.6	64.9
Length anal-fin base	27.8	30.4	31.2	31.1	28.5	31.6	31.3	30.2	29.1	30.8
Length pectoral fin	29.7	29.8	29.6	29.4	31.7	31.6	30.7	31.8	31.3	32.6
Length pelvic fin	32.9	35.9	34.4	34.6	33.6	38.3	36.5	38.3	39.7	36.5
Length pelvic-fin spine	17.6	19.8	18.3	18.1	18.6	19.5	18.6	21.3	20.7	19.4
Length first dorsal spine	9.4	8.6	10.1	8.9	9.2	8.4	9.2	9.8	9.1	8.8
Length seventh dorsal spine	15.6	16.4	14.3	15.3	17.3	17.9	17.1	18.2	17.1	17.9
Length last dorsal spine	18.3	18.4	0.0	18.2	17.8	20.0	18.1	19.3	19.9	19.5
Length longest dorsal ray	26.5	24.4	29.2	27.4	22.8	25.4	30.1	23.4	25.8	24.9
Length first anal spine	7.4	8.7	9.2	8.2	8.4	9.4	10.1	10.3	8.9	8.4
Length second anal spine	16.1	18.5	16.6	18.2	18.6	18.5	17.3	20.2	20.0	17.4
Length longest anal ray	23.0	23.6	26.1	23.9	18.9	23.0	26.6	22.9	23.5	23.7
Length caudal fin	34.9	32.9	38.5	35.9	34.1	36.1	45.9	35.0	34.2	36.5
Caudal concavity	12.9	9.3	19.2	8.3	11.4	9.4	16.9	8.8	10.1	9.0





**Figure 2.** *Pomacentrus andamanensis* n. sp., preserved holotype, 64.3 mm SL, Surin Islands, Thailand (G.R. Allen).

**Color in alcohol.** (Fig. 2) Generally tan with slightly yellowish fins; dark brown to blackish spot near lateral-line origin and upper base of pectoral fin; a pale-edged black spot on middle of rear dorsal fin.

**Etymology.** The specific epithet refers to the native range in the Andaman Sea and is treated as a masculine geographic adjective.

**Distribution.** The new species occurs on coral reefs of the Andaman Sea (Fig. 3), including the Andaman Islands, Myanmar (Mergui Archipelago), west coast of Thailand (including Similan and Surin Islands), and the northwestern tip of Sumatra (Pulau Weh). The depth range is from about 2–35 m, but it is most commonly seen in less than 15 m.

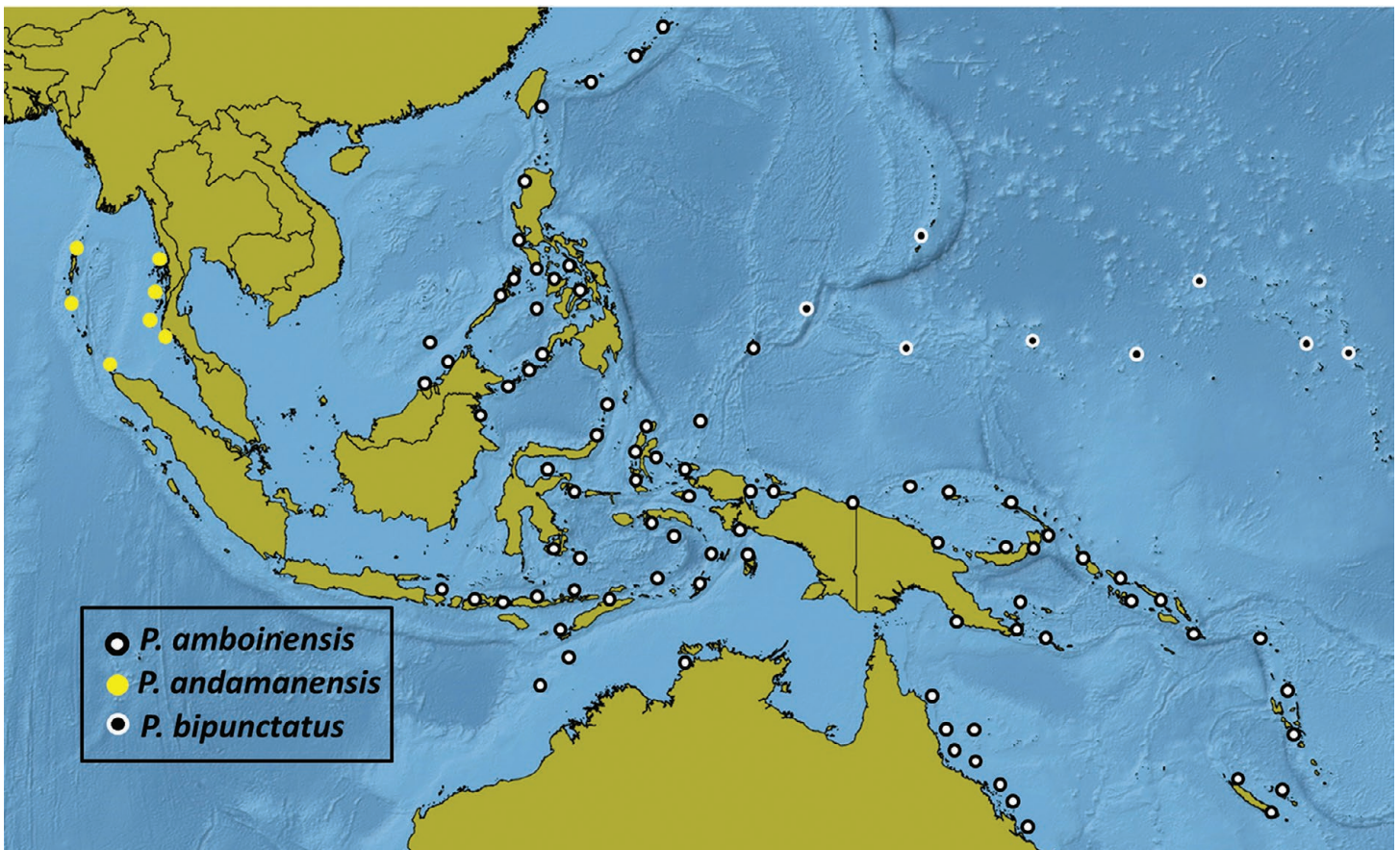


**Figure 3.** Geographic distribution of members of the *Pomacentrus amboinensis* species complex.



TABLE 2

Meristic values for the *Pomacentrus amboinensis* species-complex

	Dorsal-fin soft rays					Anal-fin soft rays				Pectoral-fin rays			
	13	14	15	16		14	15	16		16	17	18	19
<i>P. amboinensis</i>	1	12	19	1		2	29	2		9	49	8	
<i>P. andamanensis</i>		21	10			4	26	1		3	53	5	
<i>P. bipunctatus</i>		6	15			1	12	8			21	21	

	Lateral-line scales						Total gill-rakers					
	15	16	17	18	19		20	21	22	23	24	25
<i>P. amboinensis</i>	2	11	33	19	1				6	18	7	2
<i>P. andamanensis</i>		5	24	23	5		3	5	13	8		
<i>P. bipunctatus</i>		8	12	1	1				5	9	6	1

**Comparisons.** The new species belongs to the *Pomacentrus amboinensis* complex of species, which, in addition to the nominal species, also contains *Pomacentrus bipunctatus* Allen & Randall, 2004 from Micronesia and another putative member of this group, *Pomacentrus spilotoceps* Randall, 2002 (Fig. 4) from Fiji and Tonga, which also has the characteristic spots on the upper opercle and upper pectoral-fin base and a prominent ocellus on the rear dorsal fin of juveniles (and occasionally adults). However, the general coloration of adults is usually much darker than that of the other members of the group and the dark marking on the opercle is vertically elongate rather than round. It was described on the basis of only 4 specimens and additional material is required, as well as tissue samples for genetic analysis, in order to properly assess its relationships.

The new species replaces *P. amboinensis* in the Andaman Sea (Fig. 3). The two species share morphological attributes, and have similar coloration as well. However, there are consistent differences in color patterns of both



Figure 4. *Pomacentrus spilotoceps*, approx. 55 mm SL, Lau Group, Fiji (G.R. Allen).



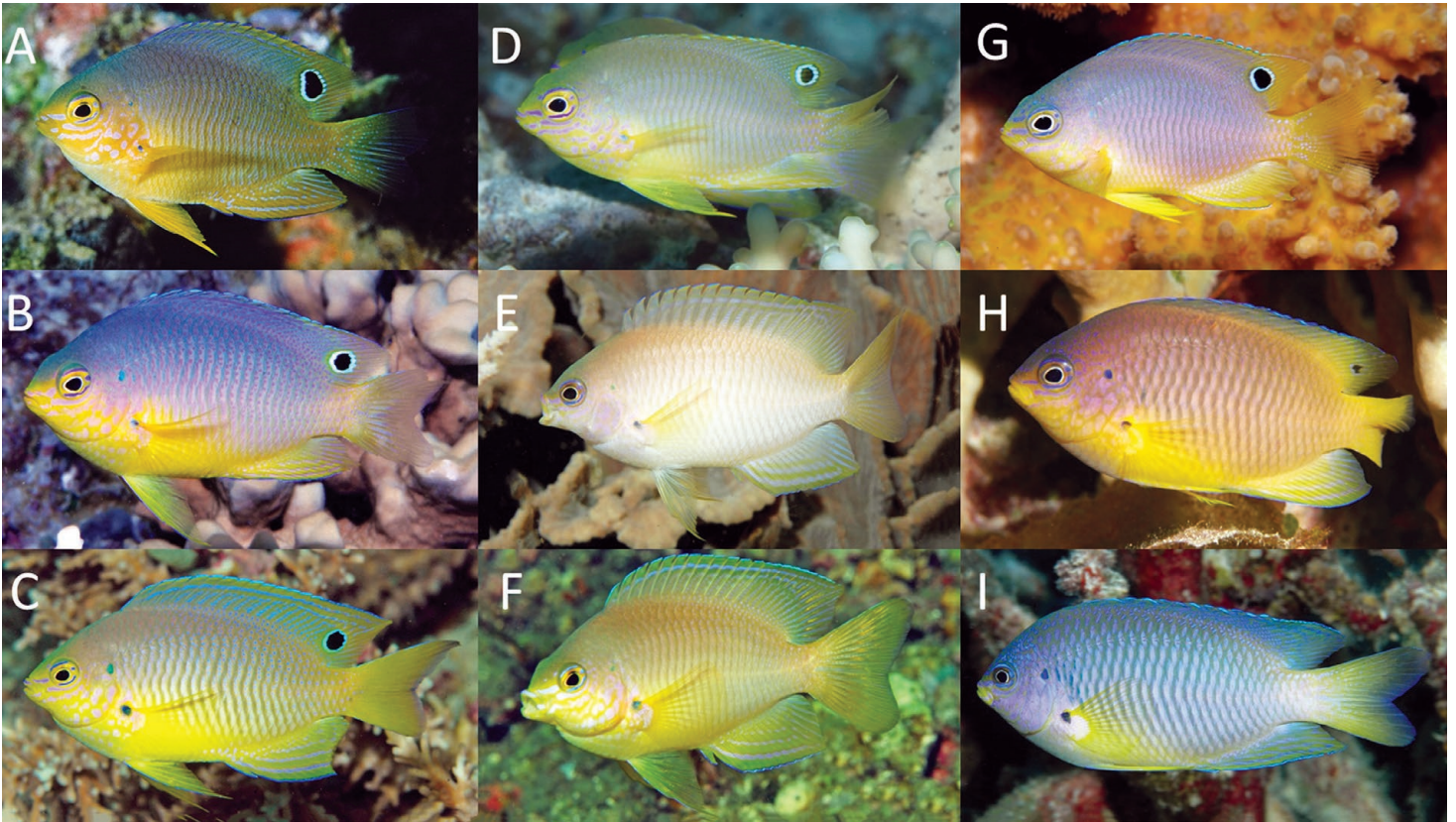


**Figure 5.** Comparative color patterns for members of the *Pomacentrus amboinensis* species group: A) *P. andamanensis*, juvenile, approx. 35 mm SL, Phuket, Thailand; B) *P. andamanensis*, subadult, approx. 45 mm SL, Andaman Islands; C) *P. andamanensis*, adult, approx. 55 mm SL, Myanmar; D) *P. amboinensis*, juvenile, approx. 35 mm SL, Milne Bay Province, Papua New Guinea; E) *P. amboinensis*, subadult, approx. 50 mm SL, West Papua, Indonesia; F) *P. amboinensis*, adult approx. 60 mm SL, Luzon, Philippines; G) *P. bipunctatus*, juvenile, approx. 30 mm SL, Ngulu Atoll, Micronesia; H) *P. bipunctatus*, subadult, approx. 45 mm SL, Pohnpei, Micronesia; and I) *P. bipunctatus*, adult, approx. 55 mm SL, Ngulu Atoll, Micronesia (G.R. Allen).

adults and juveniles (Fig. 5). An important difference is the characteristic ocellus on the dorsal fin of juveniles, which usually disappears in *P. amboinensis* between about 35–40 mm SL, up to about 45 mm SL, but is present in all growth stages, including large adults in *P. andamanensis*. Furthermore, the head and body of *P. amboinensis* ranges from pale yellow to yellowish-white, vs. brighter yellow ventrally and pale lavender to bluish gray on the upper two-thirds of body and dorsal part of the head of *P. andamanensis*. While both species have small blue to lavender spots on the body scales, these are usually more apparent in *P. amboinensis* juveniles under about 40 mm SL and are either inconspicuous or absent in adults, vs. relatively conspicuous at all growth stages in *P. andamanensis*. The two species generally share other aspects of the color pattern, including blue eye-stripes, lavender markings on the head, the greenish “ear” spot on the upper opercle, and a small dark spot at the base of the upper pectoral-fin base. Meristic features (Table 2) are about the same with the exception of a modal difference in the total rakers on the first gill arch: the mean for 29 specimens of *P. andamanensis* was 21.9 (72% with 22 or fewer rakers) compared to a mean of 23.2 (82% with 23 or more rakers) for 33 specimens of *P. amboinensis*.

Similarities between *P. andamanensis* and *P. bipunctatus* from Micronesia are also clearly evident. Shared color-pattern features include the lavender markings on the head and dark spots on the upper opercle and upper pectoral-fin base. However, as in *P. amboinensis*, the ocellus on the rear dorsal fin of *P. bipunctatus* disappears in larger juveniles after about 45 mm SL. In addition, *P. bipunctatus* differs from the other members of the group in possessing numerous blue spots on the forehead at all growth stages and having about equal numbers of 17 and 18 pectoral-fin rays (Table 2).

**Phylogenetics.** A well-defined sequence of 549 base-pairs of the control region mtDNA marker was obtained from 51 *P. amboinensis* and 7 *P. andamanensis* (in addition to 4 *P. moluccensis* as an outgroup). The phylogenetic



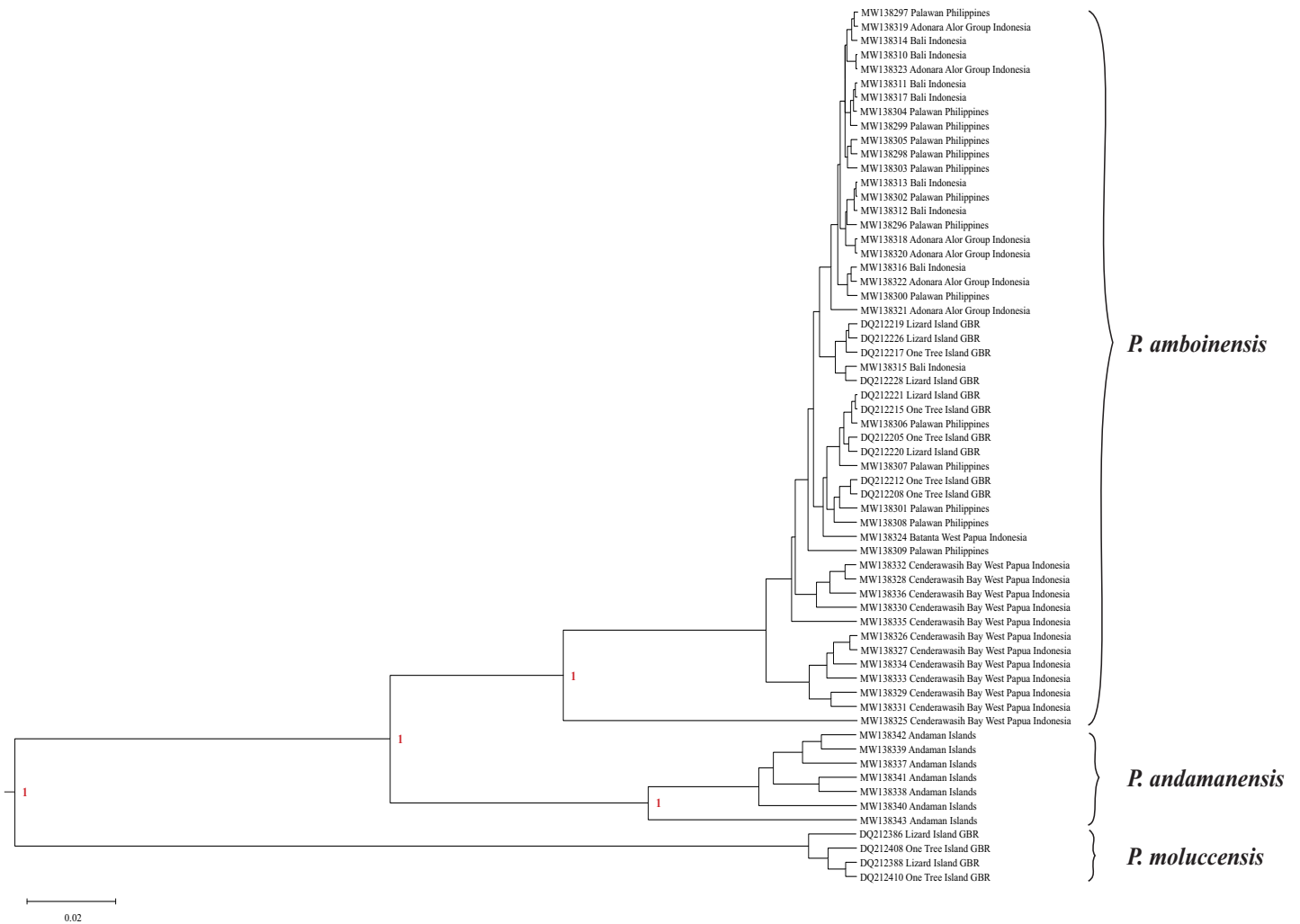


**Figure 6.** Phylogenetic tree of *Pomacentrus* control region mtDNA sequences using Bayesian Inference with HKY+G model. Genbank accession numbers and collection location are listed for each sequence. Numbers above the major nodes indicate posterior probability using the Bayesian Inference method.

**TABLE 3**

Pairwise genetic distance matrix for mtDNA control region sequences among the nine populations of *Pomacentrus* included in this study

species	location	1	2	3	4	5	6	7	8	9	10
1	<i>P. andamanensis</i> Andaman Islands										
2	<i>P. amboinensis</i> Cenderawasih Bay, W.Papua, Indonesia	0.21									
3	Adonara, Alor Group, Indonesia	0.21	0.04								
4	Batanta, West Papua, Indonesia	0.21	0.04	0.02							
5	Bali, Indonesia	0.21	0.04	0.01	0.02						
6	Palawan, Philippines	0.21	0.04	0.01	0.02	0.02					
7	One Tree Island, Australia	0.21	0.04	0.02	0.02	0.02	0.02				
8	Lizard Island, Australia	0.21	0.04	0.02	0.01	0.02	0.02	0.01			
9	<i>P. moluccensis</i> One Tree Island, Australia	0.38	0.38	0.38	0.38	0.38	0.38	0.38	0.38		
10	Lizard Island, Australia	0.38	0.38	0.38	0.38	0.38	0.38	0.38	0.38	0.01	

tree generated by BEAST (Fig. 6) reveals two distinct clades corresponding to the two species, well-separated from the outgroup species, *P. moluccensis*, with a 100% posterior probability using the Bayesian Inference method. Pairwise genetic distances using Patristic (Fourment & Gibbs 2006) showed divergences in control region sequences between the 7 geographic populations of *P. amboinensis* ranging from 0.01–0.04, vs. 0.21 between these populations and *P. andamanensis*, and 0.38 from both to the outgroup *P. moluccensis* (outgroup) (Table 4). These results certainly support the elevation of the Andaman Islands population to species status.

**Discussion.** The relationship between *Pomacentrus amboinensis* and *P. andamanensis* is very similar to the situation for other species pairs discussed by Randall (1998). He listed 52 examples of probable geminate or twin species pairs in the East Indian region (Andaman Sea to Solomons) that evolved from former widely distributed populations that were probably isolated as a result of lowered sea levels and concomitant land barriers during past glacial periods. The former isolation of the Andaman Basin is biologically well supported by the presence of at least 20 endemic species of reef fishes (Table 3), including several species with an apparent geminate relationship similar to that of *P. amboinensis* and *P. andamanensis* (Fig. 8). Although the shallow (mainly < 50m depth) Malacca Straits now forms an obvious conduit between the Andaman Sea and South China Sea, it probably did not play an important role in the evolution of Andaman endemics. It was part of the Sunda mainland for most of its geological history, and did not form an aquatic connection until at least 10,000 years ago (Geyh et al. 1979). More likely, the ancestral Andaman Sea colonizers arrived via the Indian Ocean coast of Sundaland. Global sea levels fluctuated greatly during the Pleistocene (2.6 Ma–11.7 ka) in association with glacial cycles, culminating in maximal lowerings of 115–130 m about 17–19 ka (Hanebuth et al. 2000, Haq et al. 2008, Ludt & Rocha 2015). Fluctuations of this magnitude would have enhanced the isolation of the Andaman Sea Basin, resulting in land barriers in all directions, including the northwest, which was blocked by emergent land extending from the present Irrawaddy Delta to the southern Andaman Islands. The only outlets were the deepwater passages of the Nicobar Islands. The extensive shallow depths of the current South China and Java seas formed emergent land during Pleistocene glacial periods, and even today this area supports an impoverished reef fish fauna (Allen & Erdmann 2012) that is seriously restricted by heavy siltation from freshwater runoff. Although the former Sundaland shoreline is now awash by shallow seas, it apparently persists as a barrier for the westward dispersal of many reef fishes. More collections are needed for confirmation, but *P. amboinensis* apparently does not occur in these shallow seas, resulting in a substantial geographic gap between it and the range of *P. andamanensis* (Fig. 4).

**Other material examined.** *Pomacentrus amboinensis*: WAM P.27464-001, 8 specimens, 28–64 mm SL, Australia, Queensland, Great Barrier Reef, Escape Reef; WAM P.27468-016, 66 mm SL, same locality as previous lot; WAM P.29044-028, 6 specimens, 31–58 mm SL, Timor Sea, Australia, Ashmore Reef; WAM P.29713-025, 3 specimens, 39–48 mm SL, Indonesia, Lesser Sunda Islands, Flores, Maumere Bay, Pulau Besar; WAM P.30325-005, 6 specimens, 27–59 mm SL, Western Australia, Scott Reef; WAM P.30737-009, 23 specimens, 17–61 mm SL, Philippines, Tawi-Tawi Province, Sibutu Island; WAM P.31196-005, 5 specimens, 25–58 mm SL, Timor Sea, Australia, Hibernia Reef; WAM P.31416-001, 13 specimens, 12–37 mm SL, Philippines, Palawan Province, Cuyo Island. *Pomacentrus bipunctatus* (all paratypes from Marshall Islands, Enewetak Atoll except holotype): BPBM 39300 (holotype), 46 mm SL, Federated States of Micronesia, Chuuk; BPBM 17967, 2 specimens, 42–62 mm SL; BPBM 29259, 6 specimens, 19–42 mm SL; BPBM 28006, 7 specimens, 11–45 mm SL; CAS 220647, 3 specimens, 28–35 mm SL; USNM 380165, 2 specimens, 33–51 mm SL; WAM P.32354-001, 3 specimens, 51–55 mm SL.

## Acknowledgments

We are grateful for the efforts of former ROM fish curator Richard Winterbottom, who collected the majority of the type specimens of the new taxon. We also thank Erling Holm of ROM for facilitating the loan of specimens. Mark Allen (WAM) provided x-rays and curatorial assistance. The first specimens of *P. andamanensis*, including the holotype, were obtained during a 1979 expedition to the Indian Ocean with John E. Randall (BPBM) that was funded by the National Geographic Society. We were afforded more recent opportunities to investigate the Andaman Sea fish fauna due to the generosity of the late Patti Seery, owner of the adventure liveaboard ship,



*Silolona*. Thanks are also due the very accommodating and efficient crew of that vessel. We are extremely grateful to Dexter and Susan Paine and their children, Mercy, Honor, and Sam, for wonderful companionship and financial assistance during several cruises aboard *Silolona*. We are especially appreciative of the continued support of our research by the Paine Family Trust. Finally, we would also like to thank Dian Pertiwi, Dita Cahyani, Andrianus Sembiring, Astria Yusmalinda, and Danie al Malik for their guidance in the genetic analysis. The manuscript was reviewed by David Greenfield and another referee.

## References

- Allen, G.R. (1991) *Damselfishes of the World*. Mergus Press, Hong Kong, China, 271 pp.
- Allen, G.R. & Erdmann, M.V. (2012) *Reef fishes of the East Indies. Volume II*. Tropical Reef Research, Perth, Australia, pp. 425–856.
- Bay, L.K., Crozier, R.H. & Caley, M.J. (2006) The relationship between population genetic structure and pelagic larval duration in coral reef fishes on the Great Barrier Reef. *Marine Biology*, 149 (5), 1247–1256.
- Fourment, M., & Gibbs, M.J. (2006) PATRISTIC: a program for calculating patristic distances and graphically comparing the components of genetic change. *BMC Evolutionary Biology*, 6 (1), 1–5.
- Fricke, R., Eschmeyer, W.N. & Fong, J.D. (Eds.) (2020a) *Eschmeyer's catalog of fishes: family/subfamily, electronic version*, San Francisco, CA, USA. Available at <http://researcharchive.calacademy.org/research/ichthyology/catalog/SpeciesByFamily.asp> (last accessed 3 December 2020).
- Fricke, R., Eschmeyer, W.N. & van der Laan, R. (Eds.) (2020b) *Eschmeyer's Catalog of Fishes: Genera, Species, References, electronic version*, San Francisco, CA, USA. Available at <http://researcharchive.calacademy.org/research/ichthyology/catalog/fishcatmain.asp> (last accessed 1 May 2020).
- Geyh, M.A., Kudrass, H.-R. & Streif, H. (1979) Sea-level changes during the late Pleistocene and Holocene in the Strait of Malacca. *Nature*, 278, 441–443.
- Guindon, S. & Gascuel, O. (2003) A simple, fast and accurate method to estimate large phylogenies by maximum-likelihood. *Systematic Biology*, 52 (5), 696–704.
- Hanebuth, T.J.J., Voris, H.K., Yokoyama, Y., Saito, Y. & Okuno, J. (2011) Formation and fate of sedimentary depocentres on Southeast Asia's Sunda Shelf over the past sea-level cycle and biogeographic implications. *Earth-Science Reviews*, 104, 92–110.
- Haq, B.U., Hardenbol, J. & Vail, P.R. (2008) Chronology of fluctuating sea levels since the Triassic. *Science*, 235, 1156–1166.
- Kumar, S., Stecher, G., Li, M., Knyaz, C. & Tamura, K. (2018) MEGA X: Molecular Evolutionary Genetic Analysis across Computing Platform. *Molecular Biology and Evolution*, 35 (6), 1547–1549.
- Lee, W.J., Howell, W.H. & Kocher, T.D. (1995) Structure and evolution of teleost mitochondrial control regions. *Journal of Molecular Evolution*, 41(1), 54–66.
- Ludt, W.B. & Rocha, L.A. (2015) Shifting Seas: the impacts of Pleistocene sea-level fluctuations on the evolution of tropical marine taxa. *Journal of Biogeography*, 42, 25–38.
- Posada, D. (2008) jModelTest: Phylogenetic Model Averaging. *Molecular Biology and Evolution*, 25, 1253–1256. doi:10.1093/molbev/msn083
- Randall, J.E. (1998) Zoogeography of shore fishes of the Indo-Pacific region. *Zoological Studies*, 37 (4), 227–268.
- Suchard, M.A., Lemey, P., Baele, G., Ayres, D.L., Drummond, A.J. & Rambaut, A. (2018) Bayesian phylogenetic and phylodynamic data integration using BEAST 1.10. *Virus Evolution*, 4 (1), vey016.
- Walsh, P.S., Metzger, D.A. & Higuchi, R. (1991) Chelex-100 as a medium for simple extraction of DNA for PCR based typing from forensic material. *Biotechniques*, 10 (4), 506–513.